

Food Engineering

Elsevier Editorial System(tm) for Journal of  
Manuscript Draft

Manuscript Number: JFOODENG-D-12-01683R1

Title: Quality and safety driven optimal operation of deep-fat frying of potato chips.

Article Type: Research Article

Keywords: deep-fat frying; acrylamide; model identification; dynamic optimization.

Corresponding Author: Dr Eva Balsa-Canto, PhD

Corresponding Author's Institution: Spanish Council for Scientific Research, CSIC

First Author: Ana Arias-Mendez, MSc

Order of Authors: Ana Arias-Mendez, MSc; Alexander Warning, MSc; Ashim K Datta, Professor; Eva Balsa-Canto, PhD

Abstract: Increasing oil temperature and heating duration in deep-fat frying of potato chips can improve textural quality but worsen the chemical safety of acrylamide formation. Optimal design of this complex process is formulated as a non-linear constrained optimization problem where the objective is to compute the oil temperature profile that guarantees the desired final moisture content while minimizing final acrylamide content subject to operating constraints and the process dynamics. The process dynamics uses a multicomponent and multiphase transport model in the potato as a porous medium taken from literature. Results show that five different heating zones offer a good compromise between process duration (shorter the better) and safety in terms of lower acrylamide formation. A short, high temperature zone at the beginning with a progressive decrease in zone temperatures was found to be the optimal design. The multi-zone optimal operating conditions show significant advantages over nominal constant temperature processes, opening new avenues for optimization.

1 Quality and safety driven optimal operation of deep-fat  
2 frying of potato chips.

3 A. Arias-Mendez<sup>a</sup>, A. Warning<sup>1</sup>, A. K. Datta<sup>1</sup>, E. Balsa-Canto<sup>a,\*</sup>  
4 *anaarias@iim.csic.es, adw88@cornell.edu, akd1@cornell.edu, ebalsa@iim.csic.es*

5 <sup>a</sup>*Bioprocess Engineering Group, IIM-CSIC, C/Eduardo Cabello 6, 36208, Vigo-Spain*

6 <sup>b</sup>*Department of Biological and Environmental Engineering, Cornell University, 208*  
7 *Riley-Robb, Ithaca, NY 14853-5701, United States*

---

8 **Abstract**

Increasing oil temperature and heating duration in deep-fat frying of potato chips can improve textural quality but worsen the chemical safety of acrylamide formation. Optimal design of this complex process is formulated as a non-linear constrained optimization problem where the objective is to compute the oil temperature profile that guarantees the desired final moisture content while minimizing final acrylamide content subject to operating constraints and the process dynamics. The process dynamics uses a multicomponent and multiphase transport model in the potato as a porous medium taken from literature. Results show that five different heating zones offer a good compromise between process duration (shorter the better) and safety in terms of lower acrylamide formation. A short, high temperature zone at the beginning with a progressive decrease in zone temperatures was found to be the optimal design. The multi-zone optimal operating conditions show significant advantages over nominal constant temperature processes, opening new avenues for optimization.

9 *Keywords:* deep-fat frying, acrylamide, model identification, dynamic

---

\*Corresponding author, e-mail: ebalsa@iim.csic.es, phone: 0034 986 23 19 30 (Ext:403)  
*Preprint submitted to Elsevier* *March 20, 2019*

11 **1. Introduction**

12 Frying generates tasty products that have crispy crusts, tempting aromas  
13 and visual appeal. These unique properties make fried foods a major part  
14 of the prepared foods market and therefore deep-fat frying is still one of the  
15 most important unit operations in the food processing industry.

16 Type of oil, oil temperature, and duration of cooking greatly affect the  
17 final quality attributes of fried foods. Often in literature, the quality is re-  
18 lated to the oil uptake and oil deterioration. Oil uptake occurs during frying  
19 due to replacement evaporated water by oil and during post frying when it  
20 is absorbed due to the vacuum from cooling. Hydrolysis and oxidation con-  
21 tribute to the development of rancid flavors deteriorating oil quality (Saguy  
22 and Dana, 2003).

23 Recent works showed that fried foods are a significant source of dietary  
24 acrylamide (Tareke et al., 2002; Zhang et al., 2005), an emerging factor that  
25 has been associated with cancer risk and neurotoxic effects. Although the  
26 details of acrylamide synthesis are not fully understood, the Maillard-driven  
27 generation of flavor and color in the frying process can be linked to the  
28 formation of acrylamide (Medeiros-Vinci et al., 2011).

29 The increased awareness of the consumers to the relationship between  
30 food, nutrition and health has emphasized the need to design (pre-)process  
31 conditions, product specifications and type of oil so as to improve product  
32 quality and to minimize oil uptake and acrylamide formation. In this regard  
33 some recommendations may be found in, for example, Alvarez et al. (2000);

34 Mestdagh et al. (2008); Brigatto-Fontes et al. (2011).

35 However, these recommendations are often obtained by means of response  
36 surface models thus having a number of important drawbacks due to the  
37 empirical, local and stationary nature of the simple algebraic models used.

38 A fundamental understanding of the deep-fat frying process and the appli-  
39 cation of adequate optimization techniques could lead to new equipment and  
40 operation designs that may improve safety and quality of the final product.

41 To understand the mechanisms involved in the process, mathematical  
42 models were developed, from the first attempts that included heat, moisture  
43 and fat transfer in the frying of foods (Ateba and Mittal, 1994; Moreira et al.,  
44 1995; Farkas et al., 1996) to the most recent porous media based models  
45 which also account for texture and acrylamide evolution (Halder et al., 2007;  
46 Thussu and Datta, 2012; Warning et al., 2012).

47 Bassama et al. (2012) considered, via simulation, two types of transient  
48 oil temperature profiles in order to asses the impact on the final acrylamide  
49 content. The first oil temperature profile started at a high temperature,  
50 followed by a lower one and the second frying oil temperature profile was  
51 vice-versa. Their work concludes that the first type of profile results in  
52 significant reductions on the final acrylamide content.

53 However at the time of designing processing profiles, not only should  
54 have acrylamide content been taken into account, but quality attributes and  
55 processing time. Of course solving such a problem via simulation is rather  
56 complicated, if not impossible, due to the numerous degrees of freedom and  
57 constraints. This work proposes the use of advanced model based optimiza-  
58 tion techniques (Banga et al., 2003, 2008) to design optimized frying processes

59 to ensure appropriate safety through minimized final acrylamide content and  
60 quality by guaranteeing the desired specifications in terms of color and tex-  
61 ture.

## 62 **2. Theory**

### 63 *2.1. Formulation of the optimization problem*

64 In industry, the traditional operation conditions for frying potato chips  
65 consist of immersing the chips in continuous fryers where the frying oil is  
66 held at high temperatures. The process duration is long enough (typically  
67 between 1-3 minutes) to guarantee a desired final color, texture, and a final  
68 moisture level less than 2% of the initial moisture content (Brennan, 2006).

69 The objective of the present work is to formulate and solve a general  
70 dynamic optimization problem to find the operating conditions (oil tempera-  
71 ture and process duration) that produces the desired quality attributes while  
72 minimizing the final acrylamide content. Mathematically stated as:

73

74 Find  $T_{oil}(t)$  and  $t_f$  to minimize  $c_{AA}(t_f)$  such that:

$$T_{oil_{min}} \leq T_{oil} \leq T_{oil_{max}} \quad (1)$$

$$t_f \leq t_{f,max} \quad (2)$$

$$QC(t_f) \leq 0 \quad (3)$$

$$\Phi(S_w, S_o, S_g, T, M, P, w, c_{AA}, T_{oil}, \boldsymbol{\kappa}, \boldsymbol{\xi}, t) = 0 \quad (4)$$

75 where  $T_{oil}$ ,  $t_f$ , and  $c_{AA}$  are the oil temperature, process duration, and acry-  
76 lamide content respectively. QC stands for the quality constraint defined in  
77 equation 5.

78 Equation 3 defines the constraints for quality as defined by color, texture,  
 79 and moisture content. Pedreschi et al. (2005, 2006) showed that the color  
 80 in the product during the frying process follows a first order kinetics. The  
 81 higher the red component of the color, the darker the potato and the worse  
 82 the commercial acceptance of the final product. In addition, these authors  
 83 show how acrylamide content is linearly correlated with the color at 1.8%  
 84 of the initial moisture content whereas Pedreschi et al. (2005) show a clear  
 85 correlation between the increase of acrylamide content and the increase of  
 86 redness. In this optimization work, it is assumed that the minimization of  
 87 acrylamide content also minimizes redness of the product. Regarding texture,  
 88 Thussu and Datta (2012) presented a mechanistic model to predict Young's  
 89 module development during frying. Their results suggest that there is not  
 90 critical difference in considering the texture or the moisture content to control  
 91 the process duration. Therefore, the constraint imposed in the optimization  
 92 will be related to the moisture content at the end of the process. In this  
 93 way, the solution of the equations to predict texture evolution is not really  
 94 necessary. The quality related inequality constraint now becomes:

$$M(t_f) - 2 \leq 0. \quad (5)$$

95 where  $M$  is the percentage of the final moisture content, which is intended  
 96 to be 2% or lower at the end of the process.

97 There is an additional set of constraints (Equations 4) which corresponds  
 98 to the system dynamics from the mathematical model of the process which  
 99 describes the evolution of the saturation of water, oil and vapor ( $S_w, S_o, S_g$ ),  
 100 product temperature ( $T$ ), moisture content ( $M$ ), pressure ( $P$ ), water vapor

101 mass fraction ( $\omega_v$ ) and acrylamide content  $c_{AA}$ ; the corresponding spatial  
102 and temporal derivatives, as functions of the spatial coordinates ( $\xi$ ); time  
103 ( $t$ ) and oil temperature ( $T_{oil}$ ). The vector  $\kappa$  keeps all model thermo-physical  
104 and kinetic parameters.

## 105 *2.2. Mathematical model of the process*

106 In the deep-fat frying process, water containing foodstuff is immersed into  
107 oil or fat at high temperatures (typically between 160 and 180°C, Pedreschi  
108 et al. (2005) ). The high temperature induces water evaporation and the  
109 formation of a thin crust. Due to the evaporation, the water is gradually  
110 transported to the boundary layer whereas the oil is absorbed by the food  
111 replacing some of the lost water. As soon as the transfer of water ends, the  
112 temperature inside the food starts to rise and the typical deep-frying sensory  
113 characteristics begin to develop.

114 A multiphase porous media based model describing heat, mass and mo-  
115 mentum transfer and acrylamide kinetics within a potato chip will be used.  
116 The potato chip is assumed to be a porous media where the pores are filled  
117 with three transportable phases: liquid water, oil, or gas (mixture of wa-  
118 ter vapor and air). The model considers a 2D geometry as illustrated in  
119 Figure 1, the potato chip is assumed to be cylindrical and heated from out-  
120 side therefore axi-symmetry can be assumed. The physical mechanisms and  
121 corresponding equations derivation are described in detail in Warning et al.  
122 (2012) and Halder et al. (2007). The final system of equations is presented  
123 in Appendix A.

124 It should be noted that most of the thermo-physical and kinetic param-  
125 eters present in the model may be found in the literature (see Table A.1

126 in the Appendix) but the heat transfer ( $h$ ) and the surface oil saturation  
 127  $S_{o,surf}$ . Previous works provided different parameter values for different oil  
 128 temperature values. However for the purpose of dynamic optimization either  
 129 a unique value for the parameters or a functional dependency with the oil  
 130 temperature is required. In either case, unknown model parameters have to  
 131 be identified from experimental data.

### 132 2.2.1. Model parametric identification

133 The objective of parametric identification (model calibration or param-  
 134 eter estimation) is to compute a unique value for the vector of unknown  
 135 parameters ( $\boldsymbol{\theta}$ ), which either coincides or is included in the vector  $\boldsymbol{\kappa}$ , so as  
 136 to minimize the distance among experimental data and model predictions.  
 137 In this work, this distance is quantified by the sum of the weighted squared  
 138 differences among experimental and simulated data (weighted least squares).

139 The problem is thus formulated as a non-linear constrained optimization  
 140 problem, as follows:

141 Find  $\boldsymbol{\theta} \in R^{n_\theta}$  so as to minimize:

$$J_{wlsq}(\boldsymbol{\theta}) = \sum_{i=1}^{n_e} \sum_{j=1}^{n_o^e} \sum_{k=1}^{n_{s,o}^e} q_{i,j,k} (\tilde{y}_{i,j,k} - y_{i,j,k}(\boldsymbol{\theta}))^2, \quad (6)$$

142 subject to the system dynamics plus bounds on the parameters:

$$\Phi(S_w, S_o, S_g, T, M, P, w, c_{AA}, T_{oil}, \boldsymbol{\theta}, \boldsymbol{\xi}, t) = 0 \quad (7)$$

$$\boldsymbol{\theta}_{min} \leq \boldsymbol{\theta} \leq \boldsymbol{\theta}_{max} \quad (8)$$



143 where  $n_e$ ,  $n_o^e$  and  $n_{s,o}^e$  correspond to the number of experiments, the number of  
144 observed quantities per experiment and the number of samples (in time and  
145 space) per observed quantity and experiment, respectively. The weight values  
146  $q_{i,j,k}$  quantify the relative importance that is assigned to a given experimental  
147 data.  $\theta_{min}$  and  $\theta_{max}$  correspond to the minimum and maximum acceptable  
148 value for the parameters.  $\tilde{y}_{i,j,k}$  corresponds to a given experimental data and  
149  $y_{i,j,k}$  corresponds to the model prediction. Hence, 6 represents the result of  
150 simulating the model and evaluating the measured quantities at sampling  
151 time  $k$  under the experimental conditions  $e$ . The observed quantities in this  
152 case correspond to the acrylamide, moisture Eq. 9 and oil content Eq. 10:

$$M(t) = 100 \times \frac{1}{M(0)} \int_S \frac{S_w \rho_w \varphi}{\rho_s (1 - \varphi)} dS \quad (9)$$

$$oil(t) = \int_S \frac{S_o \rho_o \varphi}{\rho_s (1 - \varphi)} dS \quad (10)$$

153 and the parameters to be estimated are the convective heat transfer coeffi-  
154 cient ( $h$ ) and the surface oil saturation  $S_{o,surf}$ .

155 Therefore the parameter estimation problem reads:

156 Find  $h$  and  $S_{o,surf}$  to minimize:

$$J_{wlsq}(h, S_{o,surf}) = \sum_{i=1}^{n_e} \sum_{k=1}^{n_{s,AA}^e} \left( \frac{\tilde{c}_{AA_{i,k}} - c_{AA_{i,k}}}{\max(\tilde{c}_{AA_i})} \right)^2 + \quad (11)$$

$$\sum_{i=1}^{n_e} \sum_{k=1}^{n_{s,M}^e} \left( \frac{\tilde{M}_{i,k} - M_{i,k}}{\max(\tilde{M}_i)} \right)^2 + \sum_{i=1}^{n_e} \sum_{k=1}^{n_{s,o}^e} \left( \frac{\tilde{oil}_{i,k} - oil_{i,k}}{\max(\tilde{oil}_i)} \right)^2 \quad (12)$$

$$(13)$$

157 subject to:

$$\Phi(S_w, S_o, S_g, T, M, P, w, c_{AA}, T_{oil}, h, S_{o,surf}, \boldsymbol{\xi}, t) = 0 \quad (14)$$

$$40 \leq h \leq 160(Wm^{-2}K^{-1}) \quad (15)$$

$$0.055 \leq S_{o,surf} \leq 0.22 \quad (16)$$

158 The weights  $q_{i,j,k}$  were selected so as to take into account the different orders  
 159 of magnitude of the observed quantities.  $n_{s,AA}^e$ ,  $n_{s,M}^e$  and  $n_{s,o}^e$  correspond  
 160 to the number of sampling points for acrylamide, moisture and oil content,  
 161 respectively, for the experiment  $e$ . The total amount of experimental data  
 162 used is represented as  $N_d$ .

163 In order to assess the quality of the parameter estimates, several possibil-  
 164 ities exist (Walter and Pronzato, 1997). Bootstrap or jack-knife approaches  
 165 allow to compute robust confidence intervals. However, the associated com-  
 166 putational cost make it difficult to use these methods for large scale models.  
 167 Alternatively, confidence intervals may be obtained through the covariance  
 168 matrix. The confidence interval of a given parameter  $\boldsymbol{\theta}_i^*$  is then given by:

$$\pm t_{\alpha/2}^\gamma \sqrt{\mathbf{C}_{ii}} \quad (17)$$

169 where  $t_{\alpha/2}^\gamma$  is given by Student's t-distribution,  $\gamma = N_d - n_\theta$  corresponds to  
 170 the number of degrees of freedom and  $\alpha$  is the  $(1-\alpha)$  100% confidence interval  
 171 selected, typically 95% is used.

172 For non-linear models, there is no exact way to obtain  $\mathbf{C}$ . Therefore  
 173 the use of first or second order approximations to the function  $J_{wlsq}$  in the  
 174 vicinity of the optimal solution  $\boldsymbol{\theta}_i^*$  has been suggested to compute covariance  
 175 matrix estimations. The Crammèr-Rao inequality establishes that under

176 certain assumptions on the number of data and non-linear characters of the  
 177 model, the covariance matrix may be approximated by the inverse of the  
 178 Fisher information matrix. The Fisher information matrix is a first order  
 179 approximation to the weighted least squares function. However, for highly  
 180 non-linear models, a first order approximation to the weighted least squares  
 181 seems inappropriate. Instead, the Hessian of the weighted least squares as  
 182 evaluated in the optimum ( $\mathbf{H}(\boldsymbol{\theta}^*)$ ) can be used to estimate the covariance  
 183 matrix as follows:

$$\mathbf{C}(\boldsymbol{\theta}^*) = \frac{2}{\gamma} J_{wlsq}(\boldsymbol{\theta}^*) \mathbf{H}(\boldsymbol{\theta}^*)^{-1} \quad (18)$$

### 184 3. Materials and methods

#### 185 3.1. Experimental data

186 For the purpose of parameter estimation data taken from the works by  
 187 Garayo and Moreira (2002) and Granda (2005) were used. The data consists  
 188 on three times series data for acrylamide, moisture and oil content obtained  
 189 at  $n_e = 3$  different oil temperatures (150, 165 and 180°C), with  $n_{s,AA}^e = 9$ ,  
 190  $n_{s,M}^e = 7$  and  $n_{s,o}^e = 9$ .

#### 191 3.2. Numerical methods

##### 192 3.2.1. Simulation

193 The equations of the model have been solved in COMSOL Multiphysics  
 194 3.5a , a commercial finite element software. The *Convection and Diffusion*  
 195 module was used to solve for water , oil , and acrylamide mass conservation  
 196 while *Maxwell-Stefan Diffusion and Convection* was used to gas mass fraction

197 and *Darcy's Law* and *Convection and Conduction* were used to solve for  
198 pressure and temperature respectively. Since the solution of the parametric  
199 identification and the dynamic optimization problems require the solution of  
200 the model hundreds of times, the spatial and temporal mesh were selected  
201 so as to offer a good compromise between the quality of the solution as  
202 compared to a dense mesh and the computational effort. The selected mesh  
203 consists of  $20 \times 10$  rectangular elements and the initial time step size is  $1e^{-6}s$   
204 being output time step of  $1s$ . This translates into a computational cost of  
205 approximately  $40 s$  to simulate  $1.5 min$  of frying process on a standard PC  
206 (4 Cores and 3.25GB RAM, processor speed of 2.83GHz).

### 207 *3.2.2. Dynamic Optimization*

208 Both the parametric identification and the process optimization problems  
209 presented in Section 2 can be formulated as non-linear programming prob-  
210 lems (NLP) with dynamic and algebraic constraints. For the case of process  
211 optimization under transient oil temperature profiles, and taking into account  
212 the distributed nature of the model at hand, the control vector parameteri-  
213 zation (CVP) approach can be used to transform the original problem into  
214 a constrained NLP. In this work, a piece-wise constant approximation of the  
215 oil temperature profile was considered, which translates, in practice, to the  
216 case where the chips are moving through different regions in the fryer that  
217 may be set at different temperatures.

218 To solve the resulting NLP problems, it is important to take into account  
219 that non-linear constrained problems may be non-convex, therefore the use  
220 of global optimization methods is required (Banga et al., 2003). In this  
221 regard, and considering that the computational effort devoted to simulation

222 is rather significant a hybrid global-local method is suggested to enhance the  
223 efficiency of the optimization process. In this work, a scatter search based  
224 approach (SSm) presented by Egea et al. (2007) has been selected since it  
225 has demonstrated to offer a good compromise efficiency-robustness in the  
226 solution of complex optimization and dynamic optimization problems (Egea  
227 et al., 2009).

228 The parametric identification problem was formulated and solved using  
229 the recently developed MATLAB toolbox AMIGO (Advanced Model Ident-  
230 tification using Global Optimization, Balsa-Canto and Banga (2011)). The  
231 control vector parameterization was implemented in MATLAB to solve the  
232 process dynamic optimization problem with SSm. In both cases, COM-  
233 SOL was called from MATLAB to perform the model simulations. Figure 2  
234 presents a schematic representation of the solution approaches for both types  
235 of problems.

## 236 4. Results and discussion

### 237 4.1. Model parametric identification

238 The parametric identification resulted in the following optimal parameter  
239 values  $h^* = 83.7 \text{ W m}^{-2} \text{ K}^{-1}$  and  $S_{o,surf}^* = 0.1377$ . The best fit is shown in  
240 Figures 3.

241 It should be noted that despite the fact that the parameters do not depend  
242 on the experiment as in previous works, the value of the cost function has  
243 improved from  $J_{wlsq} = 4.4$  to  $J_{wlsq} = 3.5$ . Figures 4 illustrate the differences  
244 between previous and current approximations in terms of the mean relative  
245 prediction error, revealing that the use of the optimal value for  $h$  and  $S_{o,surf}$   
246 results in a considerable improvement in the overall predictive capabilities of  
247 the model and enables the possibility of using the model throughout the range  
248 of operation conditions with unique values on the parameters. Following  
249 the same procedure, a functional dependency of the parameters on the oil  
250 temperature could be identified if more data became available.

251 Confidence intervals for the parameters were calculated through the Hes-  
252 sian of the weighted least squares as evaluated in the optimum (Equations 17  
253 and 18). The confidence interval around  $h$  is  $\pm 21.14 \text{ W m}^{-2} \text{ K}^{-1}$  (around the  
254 25%) and for  $S_{o,surf}$ ,  $\pm 0.0117$  (around the 9%). The weighted least squares  
255 contours in the vicinity of the optimal solution (Figure 5 reveal that the pa-  
256 rameters are highly correlated. This may be explained taking into account  
257 the low sensitivity of the states to modifications in the parameter values  
258 for the given experimental conditions. Figure 6 presents more detail about  
259 the evolution of the acrylamide, moisture and oil content together with the  
260 temperature for 10 different combinations of the parameter values within

261 the confidence region, showing how some of the curves are not distinguish-  
262 able. To improve sensitivity and thus confidence intervals further, optimally  
263 designed (Balsa-Canto et al., 2007), experiments are required.

## 264 *4.2. Process optimization*

### 265 *4.2.1. Constant processing temperature*

266 The typical industrial process at constant oil temperature was first con-  
267 sidered. The degrees of freedom are the processing temperature and the  
268 process duration. Figure 7 presents the optimal oil temperature obtained for  
269 each process duration and the predicted acrylamide content for each value of  
270 the decision variable. As expected, the lower the oil temperature the lower  
271 the acrylamide content and the longer the process.

272 Results reveal that a reduction in the oil temperature from  $180^{\circ}C$  to  
273  $150^{\circ}C$  translates into a reduction of around the 70% in acrylamide content  
274 and an increase of the 25% in the process duration. Since the process duration  
275 is critical for the production rate, and no recommendations or constraints  
276 are yet available on the maximum admissible acrylamide content, a good  
277 compromise would be to use intermediate temperature values ( $165 - 170^{\circ}C$ )  
278 during 80-85 s.

### 279 *4.2.2. Variable processing temperature*

280 Results from the previous section raise the question, is it possible to  
281 further reduce acrylamide content and process duration by manipulating op-  
282 erating conditions? The recent work by Bassama et al. (2012) shows, via  
283 simulation, that the application of a two-step temperature profile, with a

284 higher temperature at the beginning of the process may help to control acry-  
285 lamide formation in plantain.

286 The general dynamic optimization problem was solved for different max-  
287 imum process durations (80, 85, 90 and 95 seconds) and different numbers  
288 of maximum heating zones. First, the simplest case with two heating zones  
289 is considered assuming a fixed duration ( $t_1$ ) for the first heating zone. Re-  
290 sults (Table 1 and Figure 8 ) reveal that reductions of up to 16.5% can be  
291 achieved by using two different heating zones. For all cases, the optimum  
292 corresponds to using a larger temperature at the beginning of the process and  
293 a lower temperature at the end of the process. As expected, for the shortest  
294 processes, higher temperatures have to be used in order to assess the final  
295 moisture content constraint. Using higher temperatures and shorter process  
296 durations induces a significant increase on the acrylamide content. For in-  
297 stance, comparing results for processes lasting 80s and 85s, an increase of  
298 the 6% in process duration translates into an increase of around the 30% in  
299 final acrylamide content. Regarding the duration of the first heating zone,  
300 it seems reasonable to use 30 – 40 s, since the process is flexible enough to  
301 comply with the constraints and minimize acrylamide content while reducing  
302 energy consumption as compared to the case with  $t_1 = 20$  s.

303 Further improvements may be achieved if more flexibility is allowed (see  
304 Tables 2 and Figures 9 and 10). In this regard, the optimal profiles confirm  
305 that using a larger number of heating zones may improve results for shorter  
306 processes. In principle, five different heating zones offer the best compromise  
307 process duration and acrylamide reduction. Optimal profiles result in the  
308 use of a high temperature at the beginning of the process during a short



309 period of time and a gradual decrease of the temperature until the end of  
310 the process. For the longest process, the use of two heating zones is again  
311 the optimum, but note that, using shorter heating times calls for the use of  
312 higher temperatures.

## 313 5. Conclusions

314 This work presented the formulation of a general dynamic optimization  
315 problem devoted to compute the oil temperature profile that guaranties the  
316 desired moisture content while minimizing final acrylamide content subject to  
317 operation constraints and the process dynamics which is described by means  
318 of a rigorous porous media based model *taken from the literature*.

319 In a first step, the unknown model parameters were identified by means  
320 of experimental data *fitting*. The problem was formulated as a general opti-  
321 mization problem *to compute* the value of the heat transfer coefficient and the  
322 oil saturation constant that minimize the distance between the experimental  
323 data and model predictions as measured by the weighted least squares func-  
324 tion. The quality of the parameter estimates was assessed with confidence  
325 intervals obtained using the Hessian of the weighted least squares function at  
326 the optimum. *The fitted model presents satisfactory predictive capabilities*  
327 *therefore being suitable for process optimization purposes*.

328 A dynamic optimization problem was then defined to compute optimal  
329 process operation conditions. Several scenarios were tested to decide on the  
330 number of maximum heating zones and process duration. Results revealed  
331 that the simplest case, using two optimally designed heating zones, already  
332 reduces the final acrylamide content up to 16.5% when comparing with the

333 traditional operation conditions. Further improvements may be achieved if  
334 the number of heating zones is increased to 5.

335     As a general conclusion the use of a short high temperature zone at the  
336 beginning with a progressive decrease in zone temperatures was found to  
337 be the optimal design showing significant advantages over nominal constant  
338 temperature processes; thus opening new avenues for the design of industrial  
339 frying processes.

## 340 Acknowledgements

341 The authors acknowledge financial support from EU [CAFE FP7-KBBE-  
342 2007-1(212754)], Spanish Ministry of Science and Innovation [SMART-QC  
343 AGL2008-05267-C03-01], Xunta de Galicia [IDECOP 08DPI007402PR] and  
344 CSIC [PIE201270E075]. A. Arias-Méndez acknowledges financial support  
345 from the JAE-CSIC program.

## 346 References

## 347 References

- 348 Alvarez, M. D., Morillo, M. J., Canet, W. (2000). Characterization of the  
349 frying process of fresh and blanched potato strips using response surface  
350 methodology. *Eur Food Res Technol* 211(5), 320–335.
- 351 Ateba, P., Mittal, G. S. (1994). Modelling the deep-fat frying of beef meat-  
352 balls. *Int. J. Food Sci. Technol.* 29, 429.
- 353 Balsa-Canto, E., Banga, J. R. (2011). AMIGO, a toolbox for advanced model  
354 identification in systems biology using global optimization. *Bioinformatics*  
355 27(16), 2311–2313.
- 356 Balsa-Canto, E., Rodriguez-Fernandez, M., Banga, J. R. (2007). Optimal de-  
357 sign of dynamic experiments for improved estimation of kinetic parameters  
358 of thermal degradation. *J. Food Eng.* 82, 178–188.
- 359 Banga, J. R., Balsa-Canto, E., Alonso, A. A. (2008). Quality and safety  
360 models and optimization as part of computer-integrated manufacturing.  
361 *Compr. Rev. Food Sci. F* 7 (1), 168–174.

- 362 Banga, J. R., Balsa-Canto, E., Moles, C. G., Alonso, A. A. (2003). Improving  
363 food processing using modern optimization methods. *Trends Food Sci. &*  
364 *Technol.* 14(4), 131–144.
- 365 Bassama, J., Brat, P., Boulanger, R., Gnata, Z., Bohuon, P. (2012). Modeling  
366 deep-fat frying for control of acrylamide reaction in plantain. *J. Food. Eng.*  
367 113 (1), 156 – 166.
- 368 Brennan, J. G., 2006. *Food processing handbook*. Wiley-VCH, Technology  
369 and Engineering.
- 370 Brigatto-Fontes, L. C., Oliveira, F. G., Collares-Queiroz, F. P. (2011). Opti-  
371 mization of the deep-fat frying process of sweet potato chips in palm olein  
372 or stearin. *American Journal of Food Technology* 45, 348–361.
- 373 Choi, Y., Okos, M. R. (1986). Thermal properties of liquid foods - review.  
374 *Physical and Chemical Properties of Food*, (American Society of Agricul-  
375 tural Engineers, St. Joseph, MI, USA).
- 376 Egea, J. A., Balsa-Canto, E., Garcia, M. G., Banga, J. R. (2009). Dy-  
377 namic optimization of nonlinear processes with an enhanced scatter search  
378 method. *Ind. & Eng. Chem. Res.* 48 (9), 4388–4401.
- 379 Egea, J. A., Rodriguez-Fernandez, M., Banga, J. R., Marti, R. (2007). Scatter  
380 search for chemical and bio-process optimization. *J. Global Optim.* 37 (3),  
381 481–503.
- 382 Farkas, B. E., Singh, R. P., Rumsey, T. R., 1996. Modeling heat and mass  
383 transfer in immersion frying. i, model development. *Journal of Food Engi-*  
384 *neering* 29 (2), 211–226.

- 385 Garayo, J., Moreira, R. (2002). Vacuum frying of potato chips. *J. Food Eng.*  
386 55 (2), 181 – 191.
- 387 Granda, C. (2005). Kinetics of acrylamide formation in potato chips. Ph.D.  
388 thesis, Texas A&M University, USA.
- 389 Halder, A., Dhall, A., Datta, A. K. (2007). An improved, easily imple-  
390 mentable, porous media based model for deep-fat frying - part I: Model  
391 development and input parameters. *Food Bioprod. Process.* 85(C3), 209–  
392 219.
- 393 Medeiros-Vinci, R., Mestdagh, F., Meulenaer, B. D. (2011). Acrylamide for-  
394 mation in fried potato products. present and future, a critical review on  
395 mitigation strategies. *Food Chem.* DOI:10.1016/j.foodchem.2011.08.001.
- 396 Mestdagh, F., Wilde, T. D., Fraselle, S., Goert, Y., Ooghe, W., Degroodt,  
397 J. M., Verhe, R., Peteghem, C. V., Meulenaer, B. D. (2008). Optimization  
398 of the blanching process to reduce acrylamide in fried potatoes. *LWT-Food*  
399 *SCI & Technol* 41(9), 1648–1654.
- 400 Moreira, R. G., Palau, J. E., Sun, X. (1995). Deep-fat frying of tortilla chips:  
401 an engineering approach. *Food Technology* 49 (4), 146–150.
- 402 Ni, H., Datta, A. K. (1999). Heat and moisture transfer in baking of potato  
403 slabs. *Drying Technology* 17(10), 2069–2092.
- 404 Pedreschi, F., Leon, J., Mery, D., Moyano, P. (2006). Development of a  
405 computer vision system to measure the color of potato chips. *Food Res.*  
406 *Int.* 39 (10), 1092–1098.

- 407 Pedreschi, F., Moyano, P., Kaack, K., Granby, K. (2005). Color changes and  
408 acrylamide formation in fried potato slices. *Food Res. Int.* 38 (1), 1–9.
- 409 Saguy, I. S., Dana, D. (2003). Integrated approach to deep fat frying: en-  
410 gineering, nutrition, health and consumer aspects. *J. Food Eng.* 56(2-3),  
411 143–152.
- 412 Tareke, E., Rydberg, P., Karlsson, P., Eriksson, S., Tornqvist, M. (2002).  
413 Analysis of acrylamide, a carcinogen formed in heated foodstuffs. *J.*  
414 *Agricult. Food Chem.* 50 (17), 4998–5006.
- 415 Thussu, S., Datta, A. K. (2012). Texture prediction during deep frying: A  
416 mechanistic approach. *J. Food Eng.* 108 (1), 111–121.
- 417 Tseng, Y. C., Moreira, R., Sun, X. (1996). Total frying-use time effects on  
418 soybean-oil deterioration and on tortilla chip quality. *Int. J. Food Sci.*  
419 *Technol.* 31, 287–294.
- 420 Walter, E., Pronzato, L. (1997). Identification of Parametric Models from  
421 Experimental Data. Springer, Masson.
- 422 Warning, A., Dhall, A., Mitrea, D., Datta, A. (2012). Porous Media Based  
423 Model for Deep-Fat Vacuum Frying Potato Chips. *J. Food Eng.* 110 (3),  
424 428–440.
- 425 Zhang, Y., Zhang, G., Zhang, Y. (2005). Occurrence and analytical methods  
426 of acrylamide in heat-treated foods: Review and recent developments. *J.*  
427 *Chromatography A* 1075, 1 – 21.

428 **Appendix A. Mathematical model of the frying process**

429 A multiphase porous media model describing heat, mass, and momen-  
 430 tum transfer within a potato chip during atmospheric frying, based on the  
 431 formulation by Warning et al. (2012), was used in this work. Mass and  
 432 energy conservation equations include diffusive, capillary, and convective  
 433 transport. Momentum conservation was introduced by means of Darcy’s  
 434 equation. A non-equilibrium water evaporation rate and a kinetic model for  
 435 acrylamide formation based on chip temperature are also considered. Here  
 436 a brief overview of the most important model assumptions and equations  
 437 is presented. Warning et al. (2012) provides an indepth description of the  
 438 model equations.

439 *Mass conservation*

440 The following three equations solve for the liquid water, oil, and gas  
 441 saturation in the pores.

$$\frac{\partial}{\partial t}(\varphi\rho_w S_w) + \nabla(u_w\rho_w) = \nabla(D_{w,cap}\nabla(\varphi\rho_w S_w)) - I \quad (\text{A.1})$$

$$\frac{\partial}{\partial t}(\varphi\rho_o S_o) + \nabla(u_o\rho_o) = \nabla(D_{o,cap}\nabla(\varphi\rho_w S_o)) \quad (\text{A.2})$$

$$S_g = 1 - S_w - S_o \quad (\text{A.3})$$

442 To solve for the mass water vapor fraction of air and water vapor, binary  
 443 diffusion equation is used.

$$\frac{\partial}{\partial t}(\varphi\rho_g S_g \omega_v) + \nabla(u_g \rho_g \omega_v) = \nabla(\varphi S_g \frac{C^2}{\rho_g} M_a M_v D_{eff,g} \nabla x_v) + I \quad (\text{A.4})$$

$$\omega_a = 1 - \omega_v \quad (\text{A.5})$$

444 *Momentum conservation*

445 The pressure and fluid velocities are calculated using Darcy's equation  
 446 where pressure increases and decreases with the evaporation of liquid water.

$$\frac{\partial}{\partial t}(\varphi\rho_g S_g) + \nabla(-\rho_g \frac{k_{in,g}^p k_{r,g}^p}{\mu_g} \nabla P) = I \quad (\text{A.6})$$

$$u_i = -\frac{k_{in,i}^p k_{r,i}^p}{\mu_i} \nabla P \quad (\text{A.7})$$

447 *Energy conservation*

448 The temperature is calculated using effective properties as shown by  
 449 Warning et al. (2012) and where evaporation of water uses a non-equilibrium  
 450 formulation.

$$\frac{\partial}{\partial t}(\rho_{eff} c_{p,eff} T) + \nabla((\rho c_p u)_{fluid} T) = \nabla(k_{eff} \nabla T) - \lambda I \quad (\text{A.8})$$

$$I = K(\rho_{v,eq} - \rho_v) S_g \varphi \quad (\text{A.9})$$

451 *Acrylamide formation and degradation*

452 The transport of acrylimide is assumed only in the liquid water and solid  
 453 component while the rate of formation is given by Granda (2005) in A.11.

$$\frac{\partial}{\partial t} c_{AA} + \nabla(u_w S_w \varphi c_{AA}) = \nabla(D_{AA} \nabla(\{S_w \varphi + (1 - \varphi)\} c_{AA})) + r_{AA} \quad (\text{A.10})$$

$$\frac{d(c_{AA}(t))}{dt} = r_{AA} = \frac{14.9A \exp(\frac{-2625.8}{T}) \exp\{-14.9 \exp(\frac{2625.8}{T})(t - t_o)\}}{(1 + \exp\{-14.9 \exp(\frac{-2625.8}{T})(t - t_o)\})^2} \quad (\text{A.11})$$



454 *Boundary and initial conditions*

455 The top and left of the potato chip is heated as shown in Figure 1. The  
456 other boundaries of the chip are insulated and impermeable. The boundary  
457 conditions (B.C.) are then given as:

458 B.C. for eq. A.2:  $n_{w,surf} = u_w \rho_w + h_m \varphi S_w (\rho_{g,surf} \omega_{v,surf} - \rho_{v,fryer})$

459 B.C. for eq. A.3:  $S_{o,surf} = 0.145$

460 B.C. for eq. A.5:  $n_{v,surf} = u_g \rho_g \omega_v + h_m \varphi S_g (\rho_{g,surf} \omega_{v,surf} - \rho_{v,fryer})$

461 B.C. for eq. A.7:  $P_{surf} = P_{fryer}$

462 B.C. for Equation A.9:  $q_{surf} = h(T_{oil} - T) - (\lambda + c_{p,w}T)n_{w,surf} - c_{p,v}Tn_{v,surf} -$   
463  $c_{p,o}T_{oil}n_{o,surf}$

464 B.C. for Equation A.11:  $n_{AA,surf} = 0$

465

466  $S_{o,surf}$  is estimated in this work by means of multi-experiment parametric  
467 identification.

468 The initial conditions at  $t = 0$  are zero for oil saturation, zero for acry-  
469 lamide concentration, and 298 K for temperature. The initial water satura-  
470 tion is assumed to be 0.8 and the water vapor fraction is calculated as shown  
471 in Warning et al. (2012).

### 472 *Appendix A.0.3. Model parameters*

473 Input parameters are shown in Table A.3. Physical and thermal proper-  
474 ties are for a raw potato. For the this model,  $h$  and  $S_{o,surf}$  were estimated by  
475 a constant value that gave reasonable fit to the experimental moisture and  
476 oil content data respectively.

477

Figure

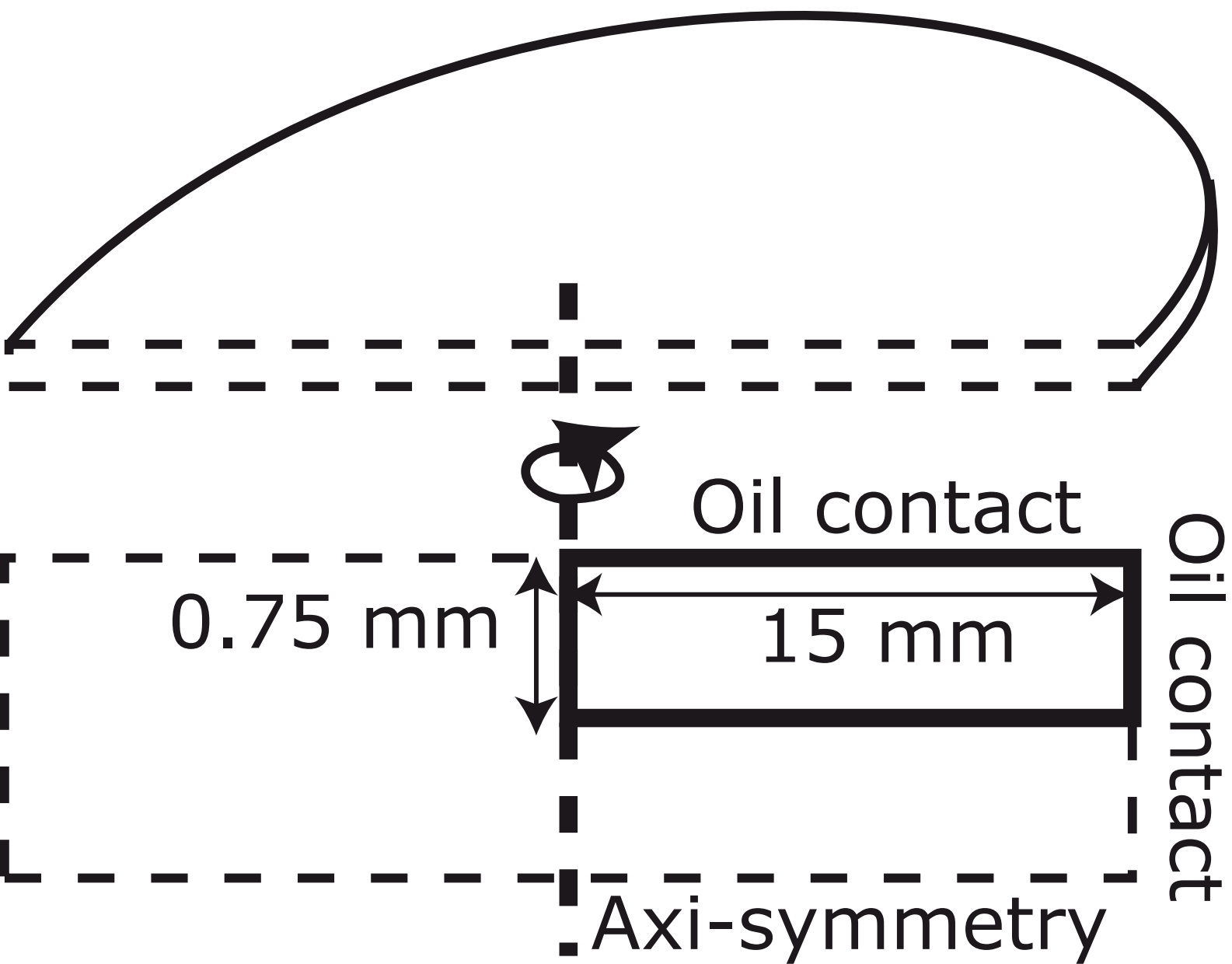
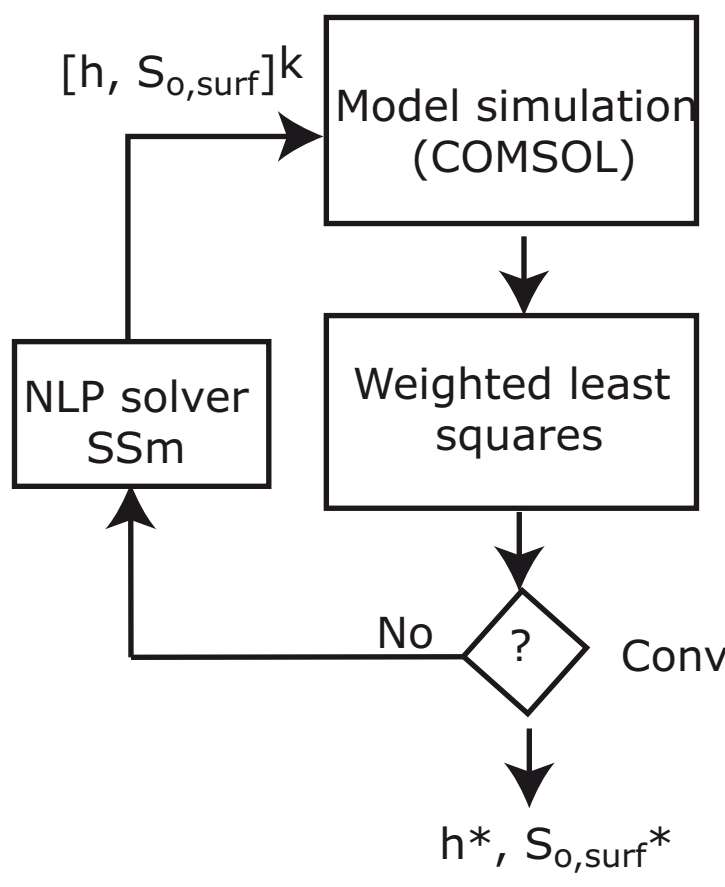


Figure2

Parametric identification (AMIGO)



Dynamic optimization (MATLAB)

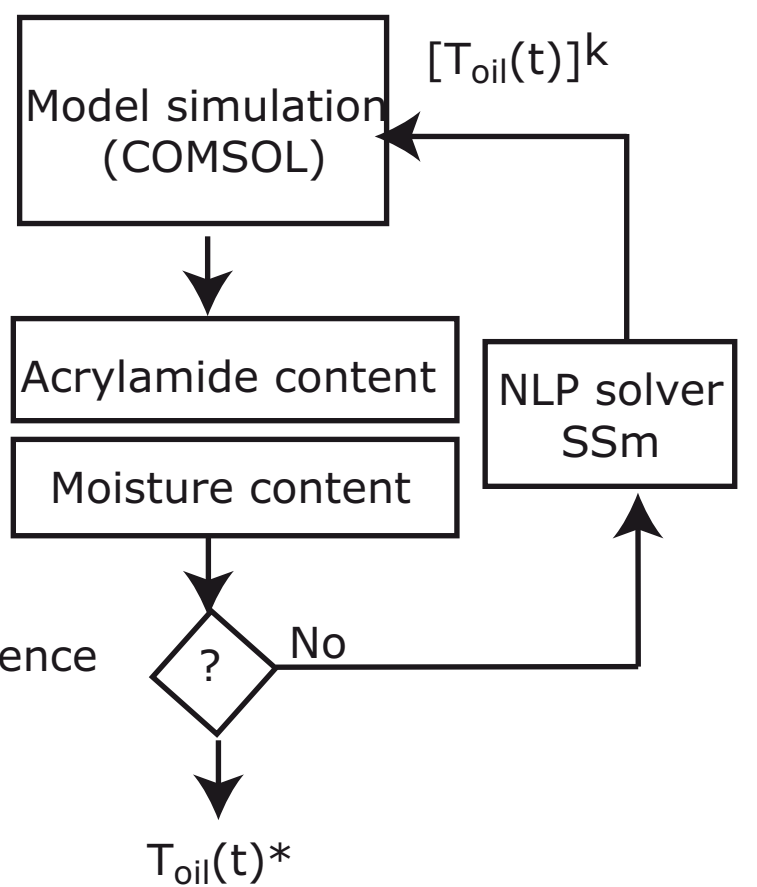


Figure3

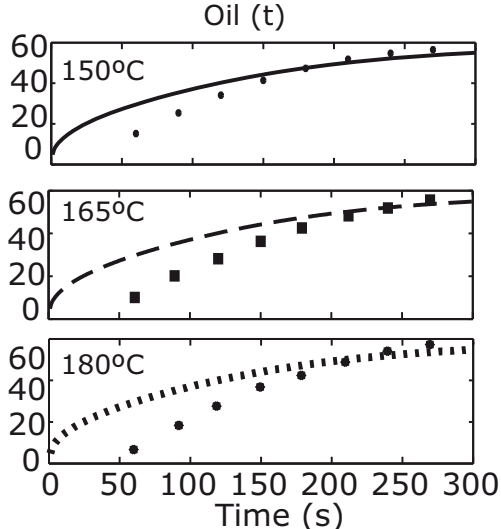
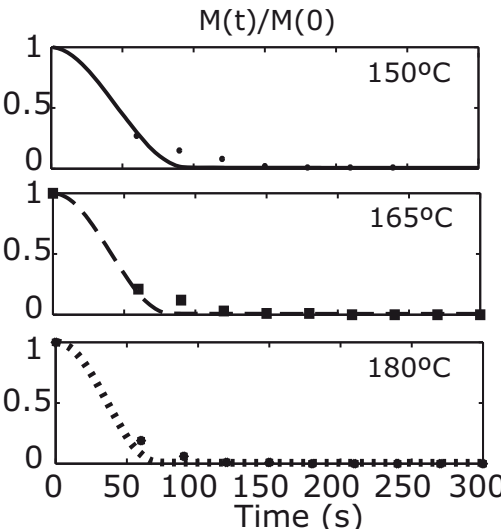
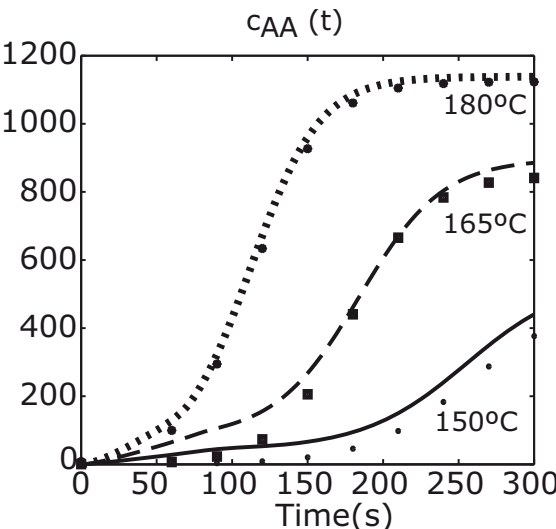


Figure4

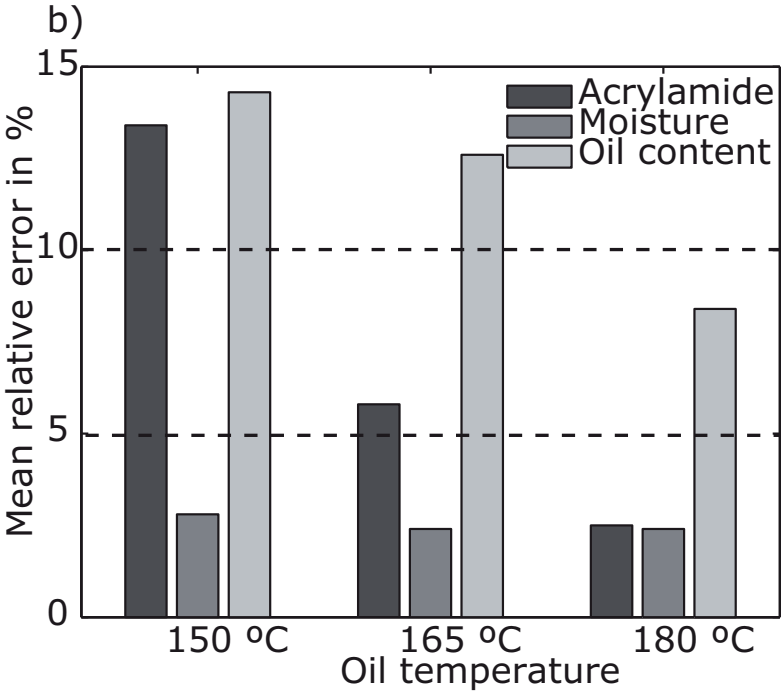
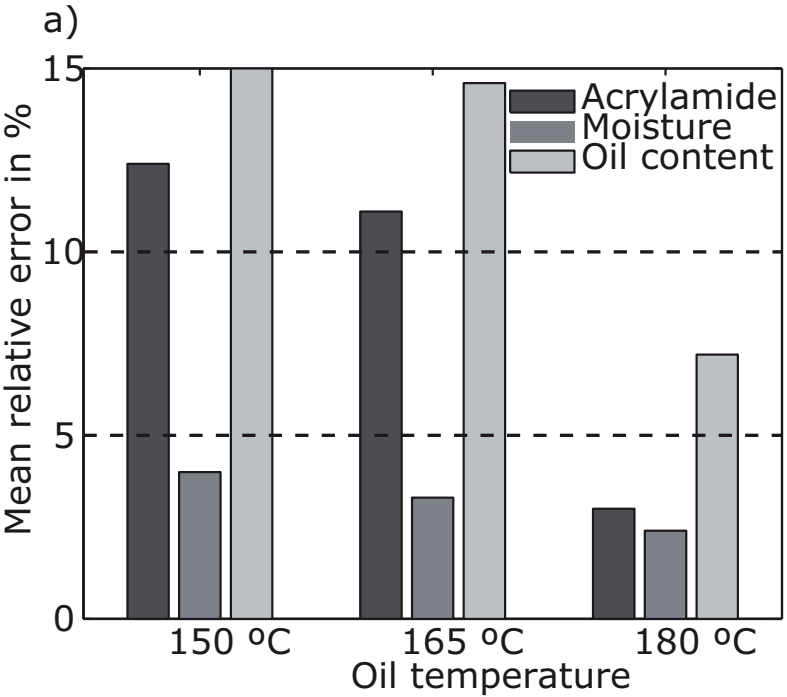


Figure5

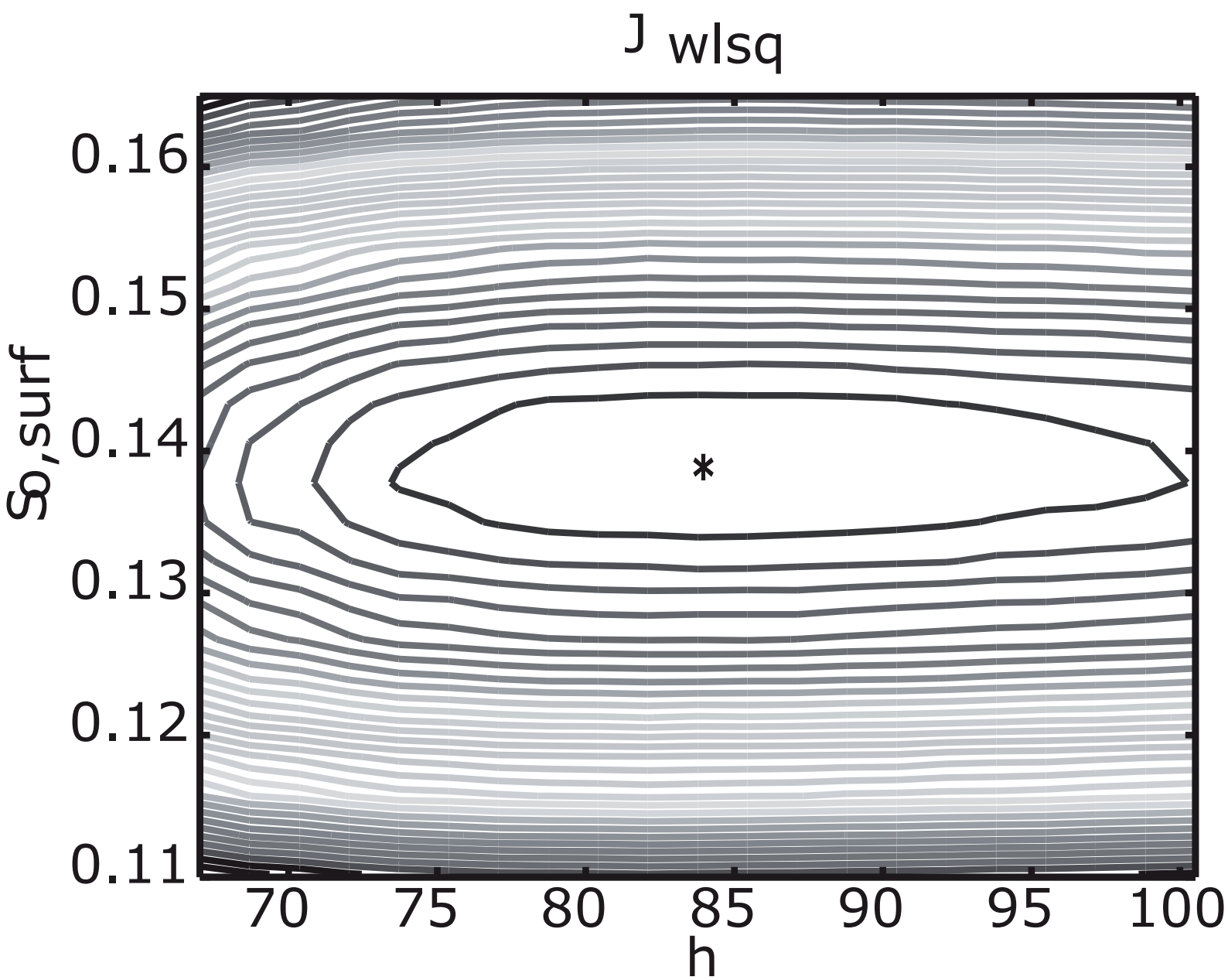


Figure6

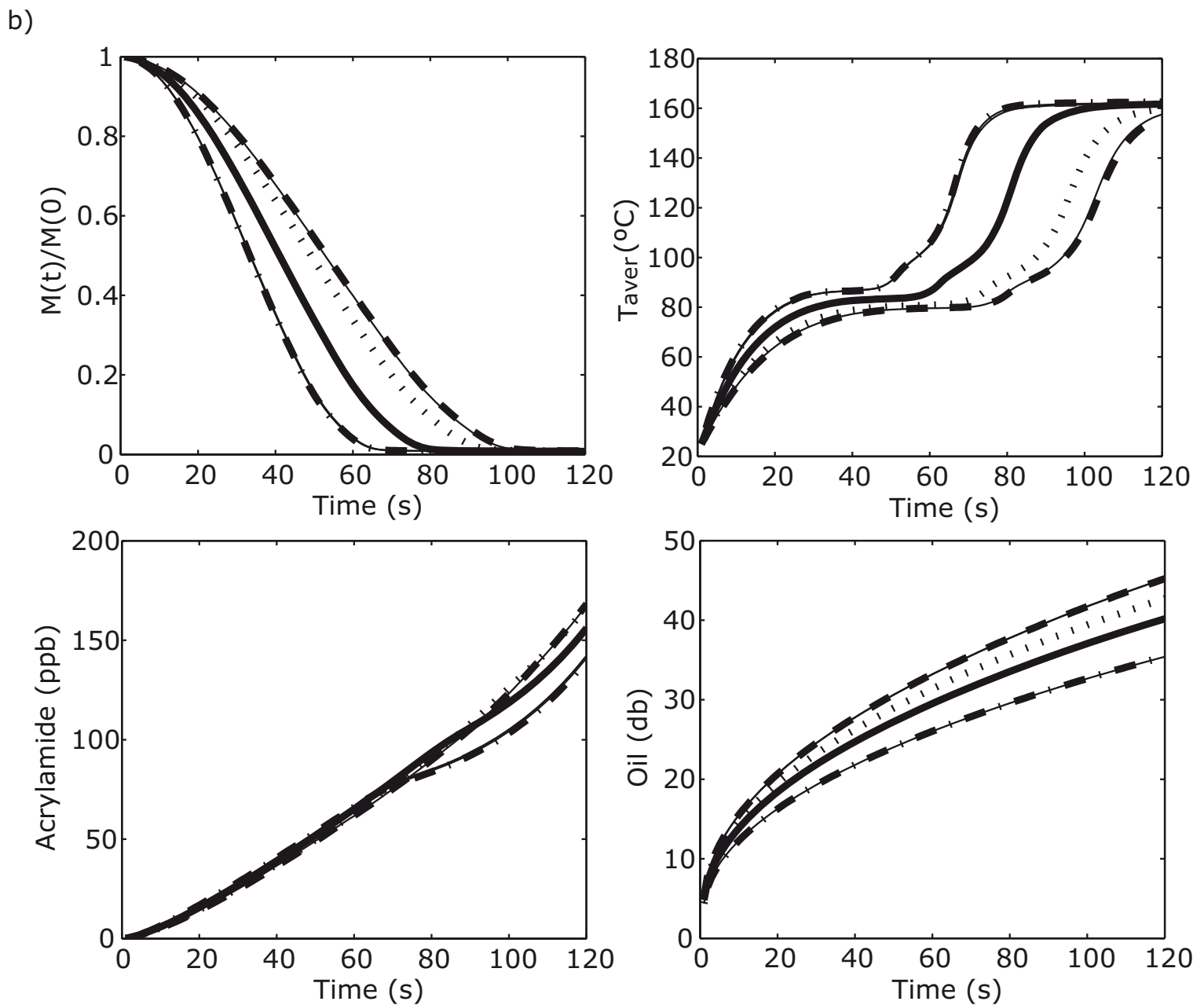
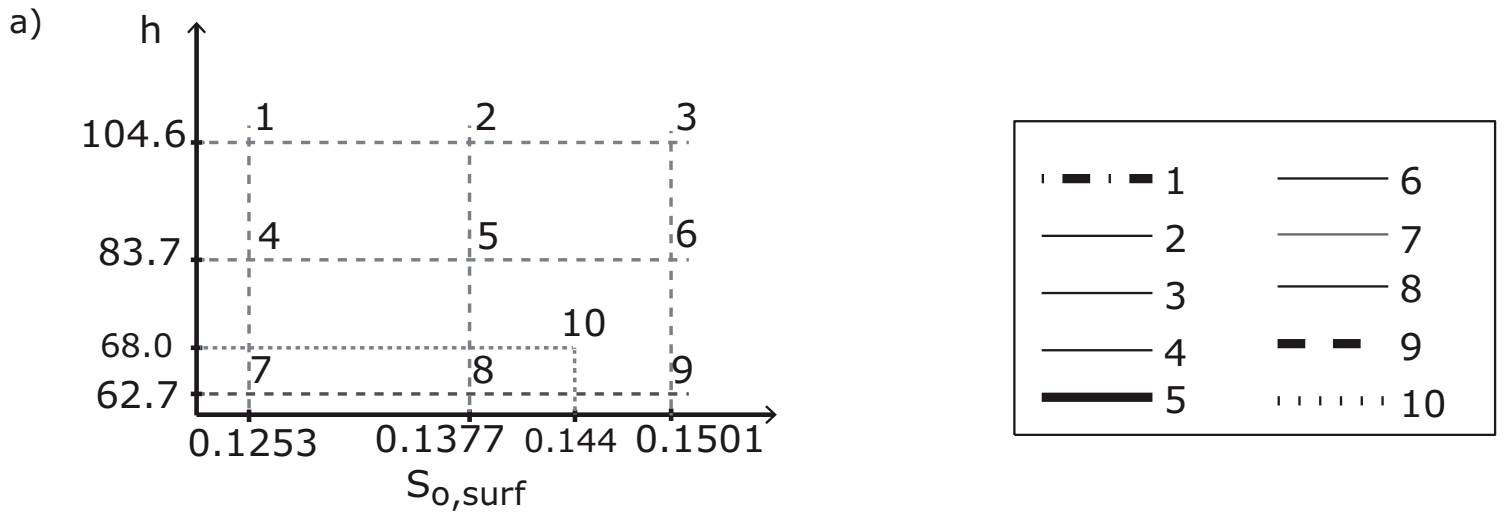


Figure7

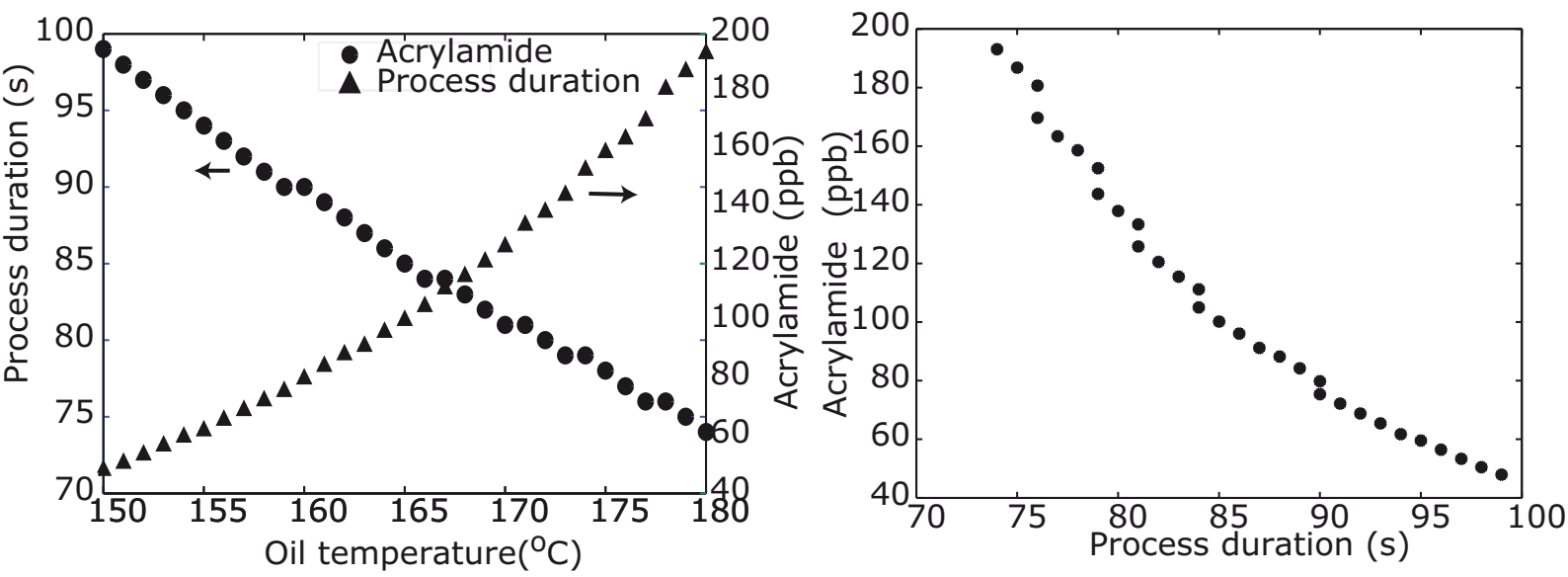
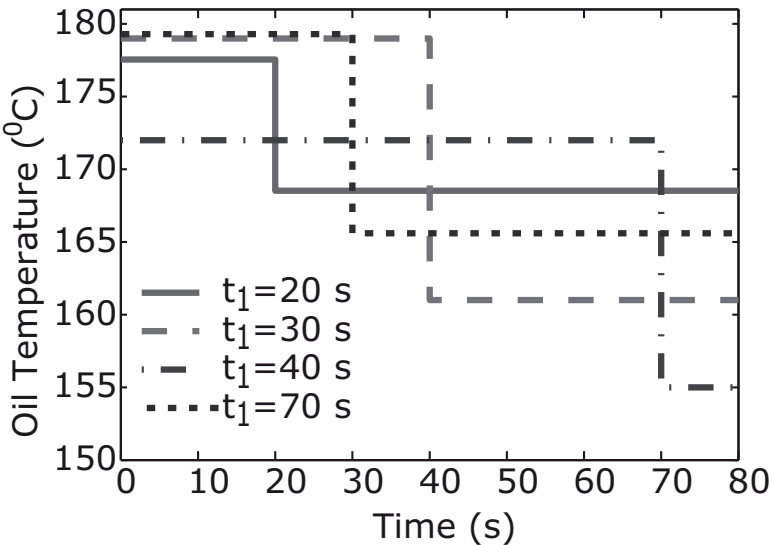


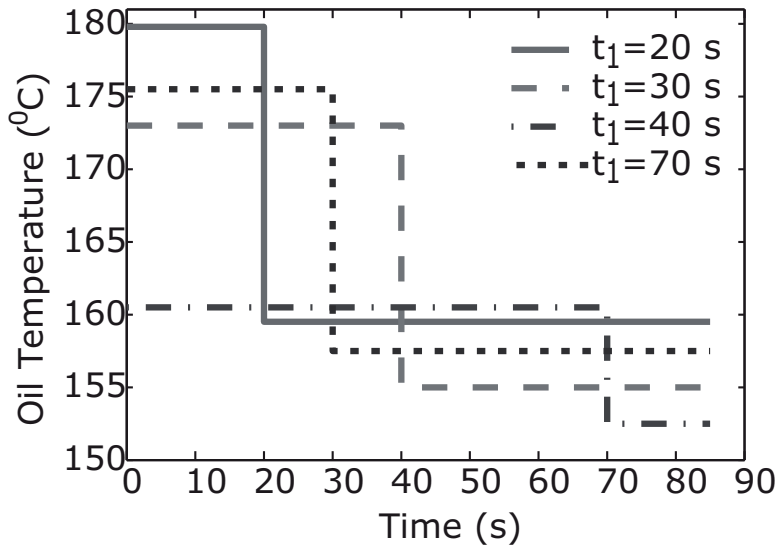


Figure8

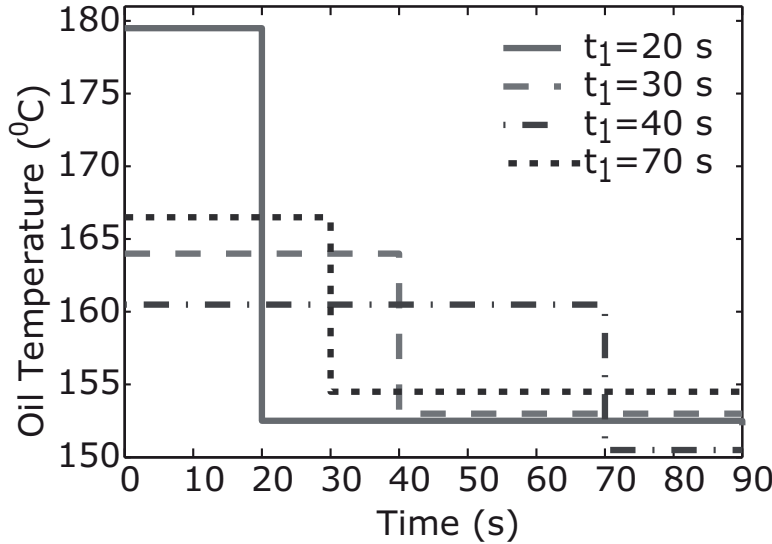
Process duration 80 seconds



Process duration 85 seconds



Process duration 90 seconds



Process duration 95 seconds

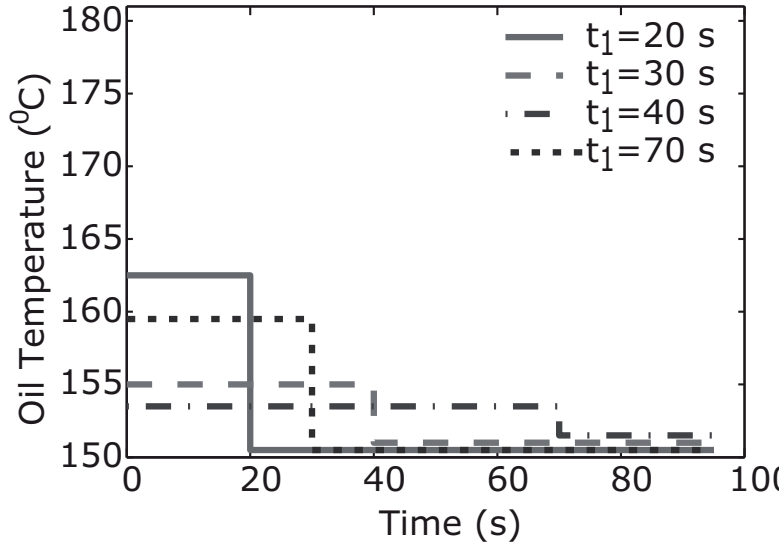


Figure9

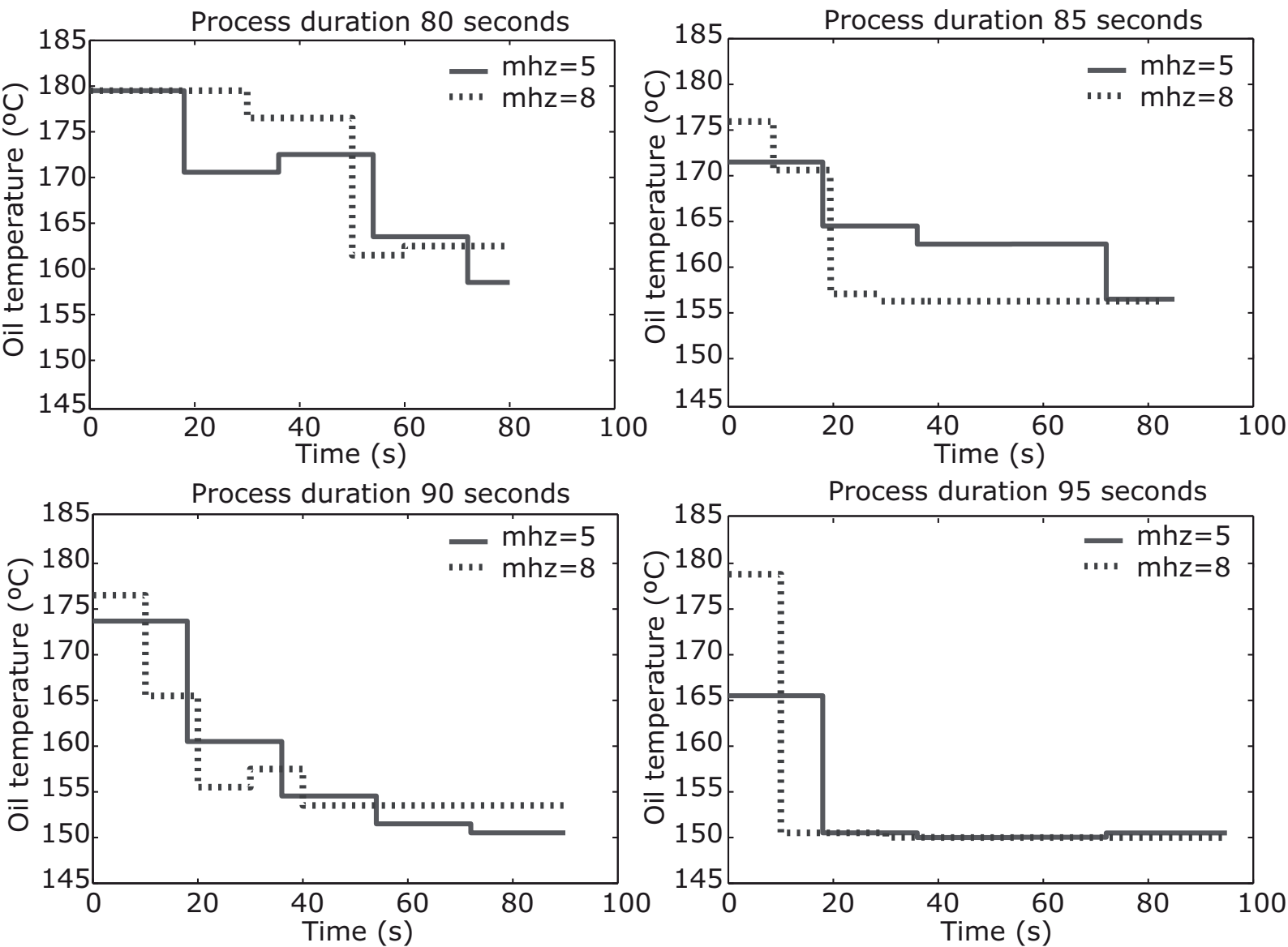
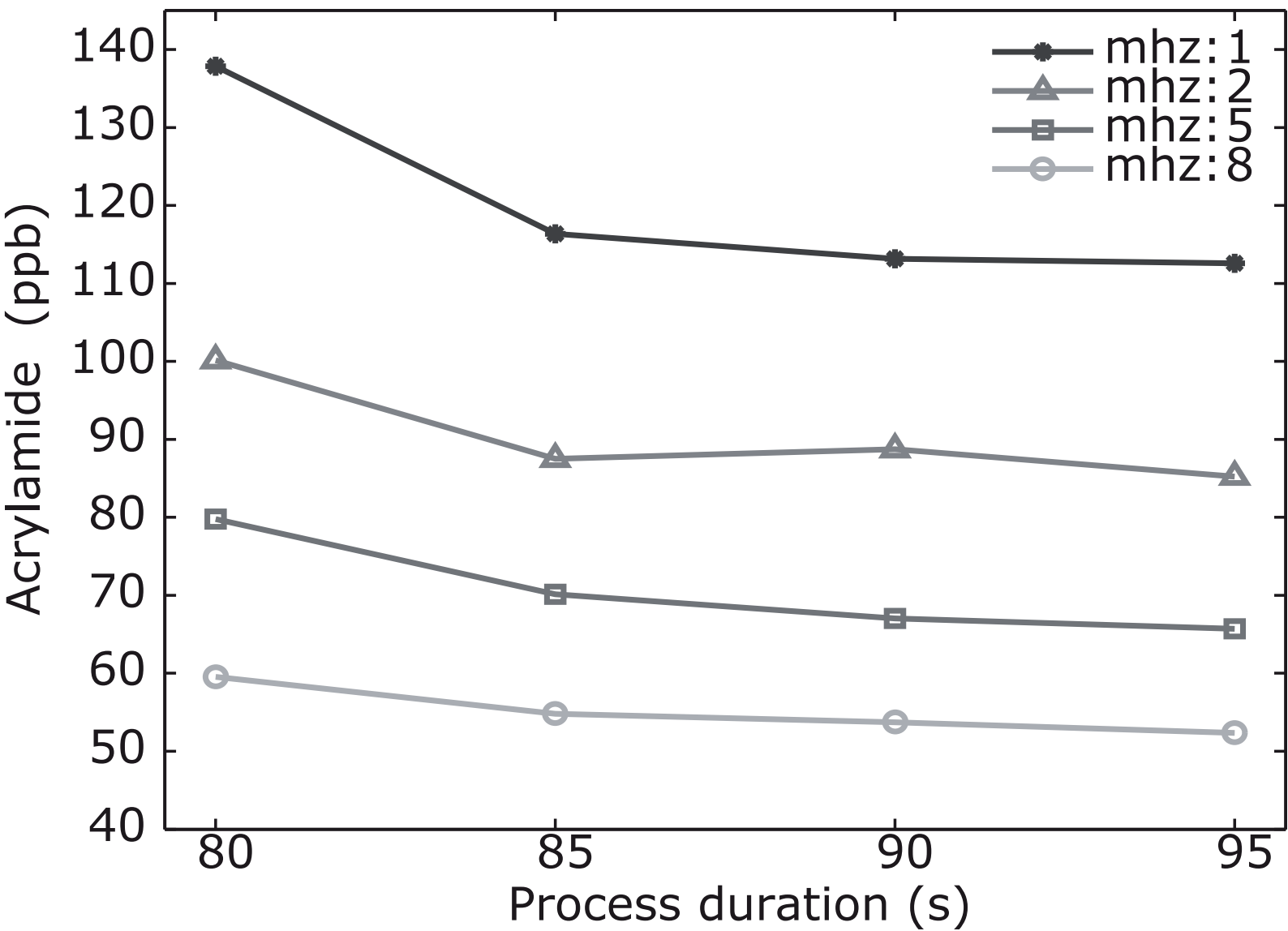


Figure10



**Figure captions**

Figure 1. 2-Dimensional computational domain and geometry of the potato chip.

Figure 2. Optimization procedures: a) Parametric identification and b) Dynamic optimization.

Figure 3. Best fit: experimental data (dots) and model data (lines) of acrylamide, oil and moisture content at different process temperatures.

Figure 4. Mean relative prediction errors: a) Model with the original set of parameters, b) Model with the optimal value of the parameters.

Figure 5. Contour plot of the  $J_{wlsq}$  in the vicinity of the optimal solution.

Figure 6. Evolution of the states for different combinations of parameter values within the confidence region.

Figure 7. Results of the process optimization problem under constant oil temperature: a) Process duration and final acrylamide content for different oil temperatures b) Pareto front.

Figure 8. Optimal oil temperature profiles for a maximum of two heating zones and different process durations.

Figure 9. Optimal operation conditions (oil temperatures) for the process using different numbers of heating zones and different maximum process durations.

Figure 10. Final acrylamide content at the optimal solutions for different numbers of maximum heating zones and process durations.

## **Highlights**

- We approach the dynamic optimization of the deep-fat frying of potato chips.
- The unknown parameters of a porous media based model are identified from data.
- The model presents good predictive capabilities and is thus used for optimization.
- We compare constant (traditional) with variable processing temperatures.
- Variable profiles maximize quality and safety while minimizing process duration.

Table 1: Final Acrylamide content at the optimal solutions (2steps).

|            | $t_{f,max}=80$ s | $t_{f,max}=85$ s | $t_{f,max}=90$ s | $t_{f,max}=95$ s |
|------------|------------------|------------------|------------------|------------------|
| $t_1=20$ s | 119.7            | 87.7             | 68.2             | 53.2             |
| $t_1=30$ s | 116.38           | 87.50            | 70.14            | 54.80            |
| $t_1=40$ s | 115.085          | 90.14            | 70.00            | 55.23            |
| $t_1=70$ s | 122.31           | 93.43            | 71.47            | 55.24            |

Table 2: Final Acrylamide content at the optimal solutions.

|       | $t_f=80$ s | $t_f=85$ s | $t_f=90$ s | $t_f=95$ s |
|-------|------------|------------|------------|------------|
| mhz=1 | 137.87     | 100.16     | 77.06      | 59.55      |
| mhz=2 | 116.38     | 87.50      | 70.14      | 54.80      |
| mhz=5 | 113.16     | 87.43      | 67.03      | 53.72      |
| mhz=8 | 112.60     | 85.24      | 65.72      | 52.35      |

## Appendix A.

Table A.3: Input parameters used in simulations.

| Parameter                 | Symbol       | Value     | Units                          | Source                 |
|---------------------------|--------------|-----------|--------------------------------|------------------------|
| Heat transfer coefficient | $h$          | 65        | $\text{Wm}^{-2}\text{K}^{-1}$  | Estimated              |
| Mass transfer coefficient | $h_m$        | Eq. 50    | $\text{m s}^{-1}$              | (Warning et al., 2012) |
| Latent heat vaporisation  | $\lambda$    | Eq. 49    | $\text{J kg}^{-1}$             | (Warning et al., 2012) |
| Porosity                  | $\varphi$    | 0.880     |                                | (Ni and Datta, 1999)   |
| Vapour diffusivity in air | $D_{eff,g}$  | Eq. 35    | $\text{m}^2\text{s}^{-1}$      | (Warning et al., 2012) |
| Evaporation constant      | $K$          | 100       | $\text{s}^{-1}$                | (Warning et al., 2012) |
| Surface oil saturation    | $S_{o,surf}$ | 0.145     |                                | Estimated              |
| Density                   |              |           |                                |                        |
| water                     | $\rho_w$     | Eq. 44    | $\text{kg m}^{-3}$             | (Warning et al., 2012) |
| vapor                     | $\rho_v$     | Ideal gas | $\text{kg m}^{-3}$             |                        |
| air                       | $\rho_a$     | Ideal gas | $\text{kg m}^{-3}$             |                        |
| oil                       | $\rho_o$     | 879       | $\text{kg m}^{-3}$             | (Tseng et al., 1996)   |
| solid                     | $\rho_s$     | Eq. 45    | $\text{kg m}^{-3}$             | (Warning et al., 2012) |
| Specific heat capacity    |              |           |                                |                        |
| water                     | $c_{p,w}$    | Eq. 36    | $\text{Jkg}^{-1}\text{K}^{-1}$ | (Warning et al., 2012) |
| vapor                     | $c_{p,v}$    | Eq. 37    | $\text{Jkg}^{-1}\text{K}^{-1}$ | (Warning et al., 2012) |
| air                       | $c_{p,a}$    | Eq. 38    | $\text{Jkg}^{-1}\text{K}^{-1}$ | (Warning et al., 2012) |
| oil                       | $c_{p,o}$    | 2223      | $\text{Jkg}^{-1}\text{K}^{-1}$ | (Choi and Okos, 1986)  |
| solid                     | $c_{p,s}$    | 1650      | $\text{Jkg}^{-1}\text{K}^{-1}$ | (Choi and Okos, 1986)  |
| Thermal conductivity      |              |           |                                |                        |
| water                     | $k_w$        | Eq. 39    | $\text{Wm}^{-1}\text{K}^{-1}$  | (Warning et al., 2012) |

|                        |              |                |                               |                        |
|------------------------|--------------|----------------|-------------------------------|------------------------|
| vapor                  | $k_v$        | 0.17           | $\text{Wm}^{-1}\text{K}^{-1}$ | (Choi and Okos, 1986)  |
| air                    | $k_a$        | 0.026          | $\text{Wm}^{-1}\text{K}^{-1}$ | (Choi and Okos, 1986)  |
| oil                    | $k_o$        | 0.026          | $\text{Wm}^{-1}\text{K}^{-1}$ | (Choi and Okos, 1986)  |
| solid                  | $k_s$        | 0.21           | $\text{Wm}^{-1}\text{K}^{-1}$ | (Choi and Okos, 1986)  |
| Intrinsic permeability |              |                |                               |                        |
| water                  | $k_{in,w}^p$ | $1 * 10^{-15}$ | $\text{m}^2$                  | (Ni and Datta, 1999)   |
| air and vapor          | $k_{in,g}^p$ | 0.17           | $\text{m}^2$                  | (Warning et al., 2012) |
| oil                    | $k_{in,o}^p$ | $1 * 10^{-15}$ | $\text{m}^2$                  | (Ni and Datta, 1999)   |
| Relative permeability  |              |                |                               |                        |
| water                  | $k_{r,w}^p$  | Eq. 41         |                               | (Warning et al., 2012) |
| air and vapor          | $k_{r,g}^p$  | Eq. 40         |                               | (Warning et al., 2012) |
| oil                    | $k_{r,o}^p$  | Eq. 42         |                               | (Warning et al., 2012) |
| Capillary diffusivity  |              |                |                               |                        |
| water                  | $D_{w,cap}$  | Eq. 32         | $\text{m}^2\text{s}^{-1}$     | (Warning et al., 2012) |
| oil                    | $D_{o,cap}$  | Eq. 33         | $\text{m}^2\text{s}^{-1}$     | (Warning et al., 2012) |
| Viscosity              |              |                |                               |                        |
| water                  | $\mu_w$      | Eq. 46         | $\text{Pa s}$                 | (Warning et al., 2012) |
| air and vapor          | $\mu_g$      | Eq. 47         | $\text{Pa s}$                 | (Warning et al., 2012) |
| oil                    | $\mu_o$      | Eq. 48         | $\text{Pa s}$                 | (Warning et al., 2012) |



## References

- Choi, Y., Okos, M. R., 1986. Thermal properties of liquid foods - review. *Physical and Chemical Properties of Food*, (American Society of Agricultural Engineers, St. Joseph, MI, USA).
- Ni, H., Datta, A. K., 1999. Heat and moisture transfer in baking of potato slabs. *Drying Technology* 17(10), 2069–2092.
- Pedreschi, F., Moyano, P., Kaack, K., Granby, K., 2005. Color changes and acrylamide formation in fried potato slices. *Food Res. Int.* 38 (1), 1–9.
- Tseng, Y. C., Moreira, R., Sun, X., 1996. Total frying-use time effects on soybean-oil deterioration and on tortilla chip quality. *Int. J. Food Sci. Technol.* 31, 287–294.
- Warning, A., Dhall, A., Mitrea, D., Datta, A., 2012. Porous Media Based Model for Deep-Fat Vacuum Frying Potato Chips. *J. Food Eng.* 110 (3), 428–440.